Cell and Tissue Research (2019) 378:279–288
https://doi.org/10.1007/s00441-019-03044-4

REGULAR ARTICLE

# Ventricular remodeling of single-chambered *myh6*$^{-/-}$ adult zebrafish hearts occurs via a hyperplastic response and is accompanied by elastin deposition in the atrium

Panagiotis Sarantis[1,2] · Catherine Gaitanaki[2] · Dimitris Beis[1]

Received: 24 July 2018 / Accepted: 7 May 2019 / Published online: 25 May 2019


## Abstract

Zebrafish (*Danio rerio*) is widely used as an animal model to understand the pathophysiology of cardiovascular diseases. Here, we present the adult cardiac phenotype of *weak atrium*, *myh6*$^{-/-}$, which carry mutations in the zebrafish atrial myosin heavy chain. Homozygous mutants survive to adulthood and are fertile despite their initial weak atrial beat. In adult mutants, the atrium remains hypoplastic and shows elastin deposition while mutant ventricles exhibit increased size. In mammals, hypertrophy is the most common mechanism resulting in cardiomegaly. Using immunohistochemistry and confocal microscopy to measure cardiomyocyte cell size, density and proliferation, we show that the enlargement of the *myh6*$^{-/-}$ ventricle is predominantly due to hyperplasia. However, we identified similar transcriptional profiles to the mammalian hypertrophy response via RT-PCR of the hyperplastic ventricles. Furthermore, we show activation of the ER-stress pathway by western blot analysis. In conclusion, we can assume, based on our model, that molecular signaling pathways associated with hypertrophy in mammals, in combination with ER-stress activation, result in hyperplasia in zebrafish. In addition, to our knowledge, this is the first time to report elastin deposition in the atrium.

**Keywords** Zebrafish · Heart · *myh6* · Hyperplasia · Hypertrophy · Elastin

## Introduction

Zebrafish is an increasingly popular animal model in biomedical research that allows modeling in vivo the underlying mechanisms of heart development, function and pathophysiology (Bakkers 2011; Bournele and Beis 2016). The physiology of the zebrafish heart resembles that of the human heart in many aspects and more than 70% of human disease genes have a clear zebrafish orthologue (Howe et al. 2013). The heart is a muscular structure, with distinct chambers and valves, which pumps oxygen-carrying blood to the organism's body in a regular, rhythmic way ensuring a consistent, unidirectional flow (Beis et al. 2005; Nemtsas et al. 2010).

We have previously characterized two mutant alleles of *myosin heavy chain 6* (*myh6*) (Kalogirou et al. 2014). *Myh6* is the atrial-specific myosin heavy chain (*Amhc*) in zebrafish. Loss of *amhc* function results in atrial contractile defects previously described as *weak atrium* (*wea*) mutants (Berdougo et al. 2003). However, *wea* mutant ventricles exhibit also an embryonic and larval phenotype, including defects in chamber circumference, wall thickness, lumen size and gene expression patterns, representing the ventricular response to a dysfunctioning atrium. In particular, enlarged ventricles and an increase in the compact ventricular myocardium were observed in *myh6*$^{-/-}$ mutant embryos indicating that atrial contractility defects also affect the ventricular morphogenesis (Auman et al. 2007).

In adult mammals, cardiac myocytes represent a highly specialized and structured cell type. Cardiac myocytes rapidly proliferate during fetal life but during the perinatal period, proliferation ceases and myocytes undergo an additional round of DNA synthesis and nuclear mitosis without proceeding to cytokinesis (acytokinetic mitosis), resulting in

✉ Dimitris Beis
dbeis@bioacademy.gr

[1] Zebrafish Disease Models lab, Center for Clinical Experimental Surgery & Translational Research, Biomedical Research Foundation Academy of Athens, 11527 Athens, Greece

[2] Department of Animal & Human Physiology, School of Biology, National and Kapodistrian University of Athens, University Campus, 157 84 Athens, Greece

binucleated adult cardiac myocytes in most species (Li et al. 1997). Typically, adult cardiac myocytes do not re-enter the cell cycle after exposure to growth signals. Instead, cardiac mass growth is achieved through an increase in cell size (Zebrowski and Engel 2013). Thus, cardiac myocytes display three distinct forms of cell cycle control and growth; namely, proliferation, binucleation and hypertrophy. On a molecular level, however, evidence is emerging of a significant overlap between the pathways regulating cell division and those driving cardiac hypertrophy (Ahuja et al. 2007; Rivello et al. 2001). Due to the original dogma that cardiomyocytes in mammals are post-mitotic cells, which cannot proliferate, it was assumed that cardiac enlargement is strictly a result of hypertrophy of cardiomyocytes and transdifferentiation of other cell types in the heart, such as fibroblasts (Anversa et al. 2006; Engel et al. 2005). Despite zebrafish being a well-recognized model in cardiogenesis research (Stainier 2001) and cardiac regeneration, it remains an underutilized organism in the study of cardiac remodeling (Chico et al. 2008). Recent publications provide strong evidence in support of zebrafish being highly relevant in modeling adult cardiomyopathies. Among ~51 known DCM causative genes, homologs of 49 genes, or 96%, were found in zebrafish (Shih et al. 2015).

Autosomal dominant mutations in human cardiac myosin heavy chain genes can result in either hypertrophic or dilated cardiomyopathy, depending on the specific gene, mutation and individual (Seidman and Seidman 2001). For example, hypoplastic left heart syndrome, which is characterized by defects in the left ventricle morphogenesis, can be the result of reduced blood flow through the left ventricle in *myh6*$^{-/-}$ caused by atrial failure (Sedmera et al. 2002). The biomechanical forces associated with contractility and blood flow have been suggested to play important roles and can trigger cardiac remodeling as well as cardiac valve morphogenesis defects as observed in *wea* mutants (Hove et al. 2003; Bartman and Hove 2005; Kalogirou et al. 2014).

The absence of a functional atrium results in ventricular overload, which can lead to the impairment of protein folding in the ER (ER-stress) and the activation of the unfolded protein response (UPR) (Glembotski 2008). Under normal conditions, the ER-resident transmembrane proteins, ATF6, inositol-requiring kinase 1 (IRE1) and PERK (dsRNA-activated protein kinase-like ER kinase), are bound with the immunoglobulin-binding protein (Bip) to maintain their inactive state (Lee 2005). When unfolded proteins accumulate in the ER, Bip dissociates from those three sensors to initiate their activity (Bertolotti et al. 2000; Wang et al. 2018). Bip was increased in hearts from patients with heart failure and hypertrophy, suggesting that UPR activation is induced in this condition (Okada et al. 2004). PERK is activated by homodimerization and autophosphorylation. The activated PERK phosphorylates Ser51 on the α-subunit of the eukaryotic initiation factor 2α (eIF2α) to prevent the formation of translational initiation complexes, which leads to attenuation of cap-dependent protein translation (Bertolotti et al. 2000).

In the context of cardiac remodeling, we also wanted to investigate what happens to the remaining atrial cells. In particular, in the zebrafish heart, structural changes are observed following damage of the myocardium and the ventricle displayed small, extending deposits of collagen in the first days post-injury (Poss et al. 2002). Collagen deposition was already reported in the atrium of *myh6*$^{-/-}$ (Kalogirou et al. 2014). In addition, using the *Tg(amhc:eGFP)*$^{s958}$ transgenic line that labels atrial cardiomyocytes, we did not observe any ectopic expression in ventricular cardiomyocytes in this model of hyperplasia, as previously shown in a model of ventricular injury (Zhang et al. 2013).

We showed that *myh6*$^{-/-}$ mutants survive to adulthood with just one functioning cardiac chamber: the ventricle. However, histological studies depicted that *myh6*$^{-/-}$ ventricles are enlarged. We set out to study the underlying mechanisms of this ventricular remodeling as a response to prolonged ventricular pressure overload and, in particular, whether they are caused by myocardial cell hypertrophy or hyperplasia and which are the associated signaling pathways. Additionally, we report the presence of elastin deposits in the site of the *myh6*$^{-/-}$ hypoplastic atrium.

## Materials and methods

### Zebrafish husbandry

Zebrafish were raised under standard laboratory conditions at 28 °C on a 14/10 h day/night cycle (Westerfield 2000). The genetic backgrounds used were the wild-type AB strain (wt) and the *myh6*$^{s459}$ mutant line (Kalogirou et al. 2014). The *myh6*$^{s459}$ line carries a recessive mutation and was identified during an ENU screen. In addition, we used *Tg(amhc:eGFP)*$^{s958}$(Zhang et al. 2013). Fish were raised in the animal facility of BRFAA (EL25BIO003) and the adult zebrafish experimental protocols were approved by the BRFAA ethics committee and the Attica Veterinary Department (no 4739).

### Ratio of ventricular area to body length calculation

Dissected hearts were imaged with a Leica DFC350FX digital camera attached to a Nikon C-DSS230 microscope. ImageJ software was used to calculate the area of the ventricle in pixels squared. The number of pixels per millimeter was calculated to convert the ventricle area in square millimeters. To determine the ventricular area to body length ratio, the ventricle area in square millimeters was divided by body length (in

mm). Body length was measured from the tip of the mouth to the body/caudal fin juncture.

## Cell size, cell density and proliferation calculation

We used ImageJ to analyze confocal stacks and determine the cell size. In order to calculate cell density, we used Imaris software (Bitplane) to achieve a three-dimensional reconstruction of the confocal z-stacks upon staining with Mef2 that marks the nucleus of cardiomyocytes. We then selected the "surpass the surface" option. At the appropriate threshold, we marked the cell nuclei and the program automatically calculates their number. We then calculated the total surface of the myocardium in each z-stack ($mm^2$). Finally, we converted the cell count in this surface to cell density (cells/$mm^2$). We calculated the proliferation of cardiomyocytes using the ratio $PCNA^+$ $MEF2^+$/total $MEF2^+$ (Sun et al. 2009; Kikuchi et al. 2011)

## Immunohistochemistry

Isolated hearts from 6-week-old and adult wild-type and *myh6*$^{-/-}$ animals were euthanized and then fixed overnight at 4 °C in 4% paraformaldehyde diluted in phosphate-buffered saline (PBS). The following day, zebrafish hearts were cryoprotected in 30% sucrose in PBS overnight. Then, the hearts were embedded in a freezing medium (Tissue-Tek OCT) and immediately frozen in liquid nitrogen. Ten-micrometer sagittal cryosections were obtained using a Leica CM3050S cryostat (Leica Microsystems). Cryosections were fixed for 5 min in 4% paraformaldehyde followed by permeabilization with 0.5% Triton-X in PBS for 5 min × 3 and blocking with 4% BSA for 1 h. For the calculation of cell size and cell density, we incubated overnight with MEF-2c (myocyte-specific enhancer factor-2c) antibody to label myocyte nuclei (1:100 Santa Cruz Biotechnology Inc.,) visualized by an anti-rabbit Alexa Fluor 633 secondary antibody (1:250, Invitrogen, Molecular Probes). For highlighting cardiac myocyte borders, we used FITC-labeled wheat germ agglutinin (WGA, Triticum vulgaris, 1:100, Sigma-Aldrich). We used elastin 2 antibody (1:100, a kind gift of Prof. Keeley) as the primary antibody visualized by anti-rabbit Alexa Fluor 568 (1:500, Molecular Probes). For the illustration of F-actin, we used Phalloidin 633 (1:250, Invitrogen, Molecular Probes). For the calculation of proliferating cardiomyocytes, we used double staining PCNA-MEF2c. We incubated cryosections for 10 min with 10% SDA, washed with PBS 3 × 5 min and with 4% BSA blocking solution for 1 h (Wang and Poss 2016). We used mouse PCNA (1:200 Sigma-Aldrich P88250) with Alexa Fluor 633 secondary antibody (1:250, Invitrogen, Molecular Probes) and anti-rabbit Alexa Fluor 488 secondary antibody (1:500, Invitrogen, Molecular Probes) for Mef-2c. The images were captured with LAS AF software on a Leica TCS SP5 inverted confocal microscope.

## Real-time PCR

Hearts from 6-week-old, wild-type and *myh6*$^{-/-}$ juveniles were excised and the ventricle was isolated. Each sample consisting of a single ventricle (six in total for each of the two groups) was frozen in TRI reagent (Sigma) using liquid nitrogen and gradually homogenized, starting with a pestle and followed by 23- and 27-gauge needles. Total RNA was extracted using TRI reagent (Sigma) according to the manufacturer's recommendations. The quantity and quality of total RNA were assessed by UV spectroscopy, by calculating the ratio of absorbance at 260 nm and 280 nm. cDNA was synthesized using Superscript III reverse transcriptase (Invitrogen). To analyze the expression level of *nppa* and *nppb*, real-time PCR was performed with SYBR Green (Molecular Probes, Life Technologies) on a Roche Lightcycler 96 (Roche Life Science). Conditions for the PCR reaction were 2 min at 50 °C and 10 min at 95 °C followed by two-step PCR for 40 cycles, each consisting of 15 s at 95 °C and 1 min at 60 °C. Real-time PCR data were converted to linear data by calculating $2^{-\Delta Ct}$ values for *18S* normalized data. The primers used were

*nppa* fw: 5′-aagcaaaagcttgtctgg
rev: 5′-actgtatccgcatattgcagc;
*nppb* fw: 5′-cattcccgtagtcggccttc
rev: 5′-cttcaatatttgccgcctttac;
*18s* fw: 5′-cacttgtccctctaagaagttgca
rev: 5′-ctgctcttcagctcgggttt.

## Western blot analysis

Hearts from wild-type and *myh6*$^{-/-}$ adult zebrafish were excised and the ventricle was isolated. Protein extraction was performed using ice-cold RIPA buffer. Proteins were resolved by electrophoresis in SDS-polyacrylamide gels (10%) on the molecular weight of each protein. Then, they were transferred to a nitrocellulose membrane (Macherey-Nagel, Germany). The membrane was blocked for 1 h at room temperature in PBST with 5% nonfat milk and then with 5% bovine serum albumin incubated with primary antibodies overnight at 4 °C. Anti-p-eif2a (Cell Signaling #9721) was used at 1:300 dilution and BiP (Cell signaling #3177) and β-actin (Abcam #ab8227) were used at 1:1000 dilution. Horseradish peroxidase-conjugated secondary antibodies (Dako) were used at 1:5000 dilution. The detection of the immunoreactive bands was performed with the Supersignal West Femto (Thermo Scientific). Relative protein amounts were evaluated by a densitometry analysis using ImageJ software. We used three independent samples for each group and β-actin for the normalization.

### Statistical analysis

*p* values were calculated with Student's *t* test and with one-way ANOVA test, using GraphPad Prism v5.01 software.

## Results

### Hypoplastic atrium and enlarged ventricles in *myh6*$^{-/-}$

The *myh6*$^{s459}$ mutant line carries an early stop codon in the *atrial myosin heavy chain* and is characterized by weak atrial contractility (Kalogirou et al. 2014). However, these mutants survive to adulthood with basically one functioning chamber: the ventricle. The mutant ventricles appear larger and more oval-shaped (Fig. 1a, b). The atria of the adult mutants are severely hypoplastic with few residual cells with atrial identity observed as denoted with the *Tg(amhc:eGFP)*$^{s958}$ (Fig. 1c, d). The ventricle area/body length ratio in wild-type is 0.032 mm$^2$/mm, significantly ($p < 0.05$, $n =$ 11 wt; 10 *myh6*$^{-/-}$) smaller than *myh6*$^{-/-}$ (0.048 mm$^2$/mm, Fig. 1e).

In order to study the characteristics of the remaining atrial cardiomyocytes and how the supply of blood directly to the ventricle is maintained, we stained for the smooth muscle marker elastin. We did not observe elastin staining in the atria of 6-week wild-type juveniles (Fig. 2a–d), but we detected significant elastin deposition flanking the residual *Tg(amhc:eGFP)*$^{s958}$-positive atrial cells of *myh6*$^{-/-}$ (Fig. 2e–h) ($n = 12$ wt; 9 *myh6*$^{-/-}$).

### The ventricle of the *myh6*$^{-/-}$ is enlarged due to hyperplasia

We then aimed to identify the mechanisms of ventricular remodeling of *myh6*$^{-/-}$ and especially to distinguish between hyperplasia or hypertrophy by estimating the cell size, cell density and proliferative potential of cardiomyocytes. We measured cell size with FITC-labeled wheat germ agglutinin (WGA) in 10 μm sagittal cryosections. In parallel, the number of cells in the section was calculated by measuring the nuclei of cardiomyocytes marked with the myocyte-specific enhancer factor-2c (MEF-2c). It is clear that unlike adult mammalian cardiomyocytes that are binuclear (Li et al. 1997; Olivetti et al. 1996), zebrafish cardiomyocytes are mononucleated (Wills et al. 2008; Foglia and Poss 2016) (Fig. 3). We did not detect any statistically significant difference in cell size measurements made in > 250 cardiomyocytes of wild-type (Fig. 3a) and *myh6*$^{-/-}$ (Fig. 3b) adults (wt = 22.20 ± 0.4289 μm$^2$ *myh6*$^{-/-}$ = 22.22 ± 0.3863 μm$^2$, Fig. 3c, $n =$ wt 18 sections from 10 hearts and *myh6*$^{-/-}$ $n = 15$ sections from 9 hearts). These findings suggest that the ventricular remodeling of *myh6*$^{-/-}$ does not involve a significant hypertrophic response.

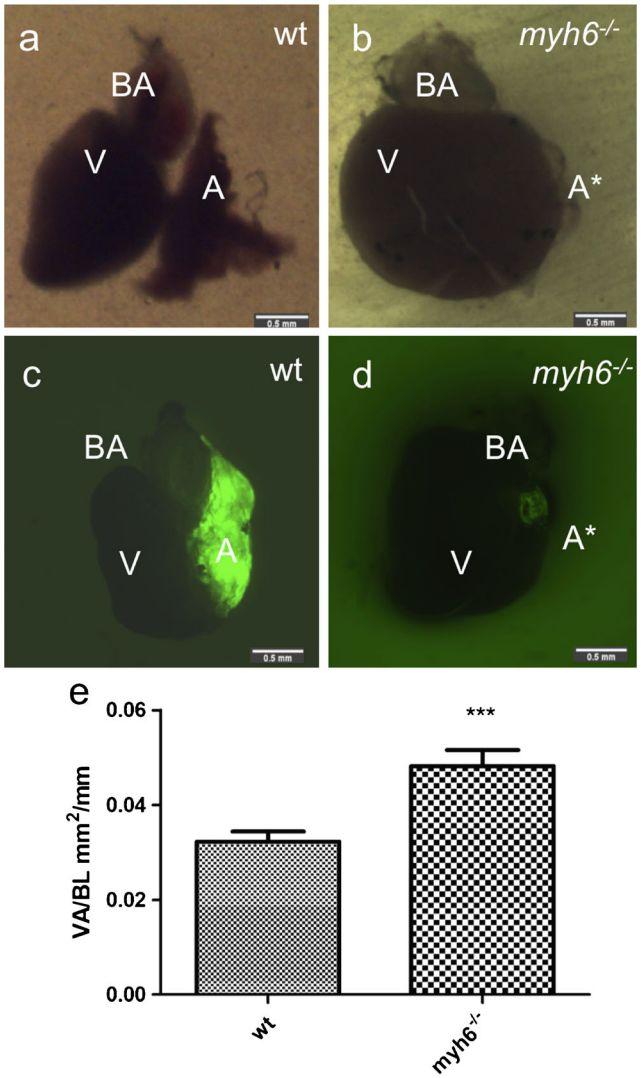


**Fig. 1** A heart from a wild-type adult zebrafish (**a**) and from a *myh6*$^{-/-}$ (**b**). *myh6*$^{-/-}$ hearts exhibit a hypoplastic atrium compared to wild-type (**c**) as shown by the amhc:egfp transgene (**d**) and an enlarged ventricle as measured from the ventricle area/body length ratio (**e**) ($p = 0.0003$). $n =$ 11 wt; 10 *myh6*$^{-/-}$). Scale bars, 0.5 mm A: atrium; V: ventricle; BA: bulbus arteriosus; A*: hypoplastic atrium

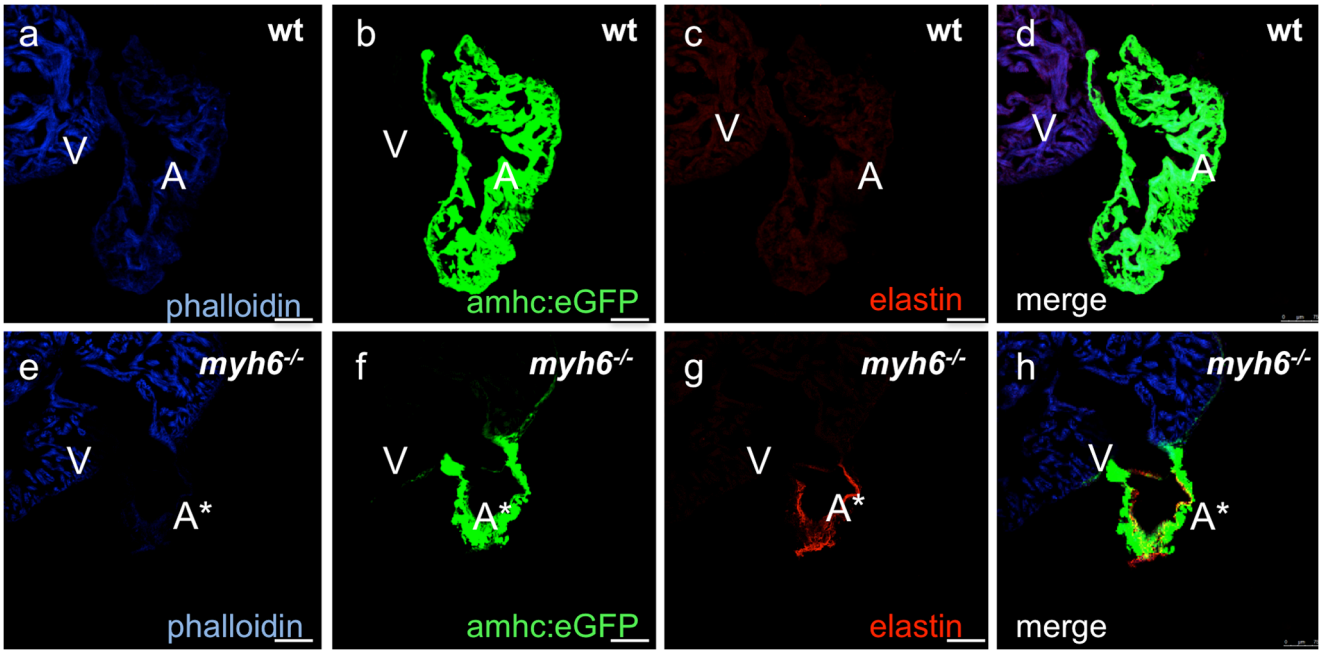


**Fig. 2** Hearts from 6-week-old wild-type zebrafish (**a**–**d**) and *myh6*$^{-/-}$ (**e**–**h**). Elastin deposition (**g**) in the hypoplastic atrium of *myh6*$^{-/-}$ is observed ($n$ = 12 wt; 9 *myh6*$^{-/-}$). Scale bars, 75 μm. A: atrium; V: ventricle; A*: hypoplastic atrium

that the cell density was significantly less in wild-type ventricles (2265 ± 74.93 cells/mm$^2$) than in *myh6*$^{-/-}$ (2804 ± 98.35 cells/mm$^2$) (Fig. 4g; $p$ = 0.0016, $n$ = 25 sections from 7 fish per group).

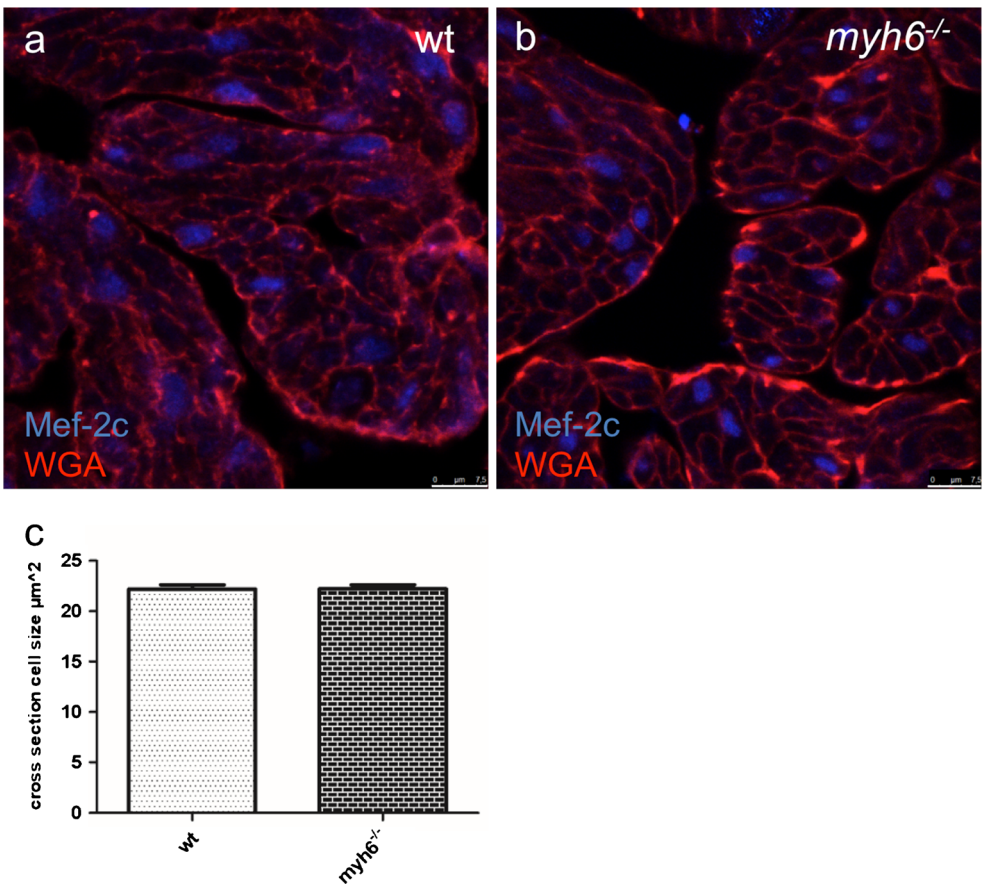


**Fig. 3** Ten-micrometer cryosections of adult zebrafish wild-type hearts (**a**) and *myh6*$^{-/-}$ (**b**). Quantification of the cardiomyocyte cell size after labeling with Mef-2c (cardiomyocytes nuclei) and WGA (cell membranes) antibodies (**c**) shows no statistically significant difference between wild-type and *myh6*$^{-/-}$. $n$ = 18 wt sections from 10 hearts and $n$ = 15 *myh6*$^{-/-}$ sections from 9 hearts. Total cells measured > 250 per sample. Scale bars, 7.5 μm

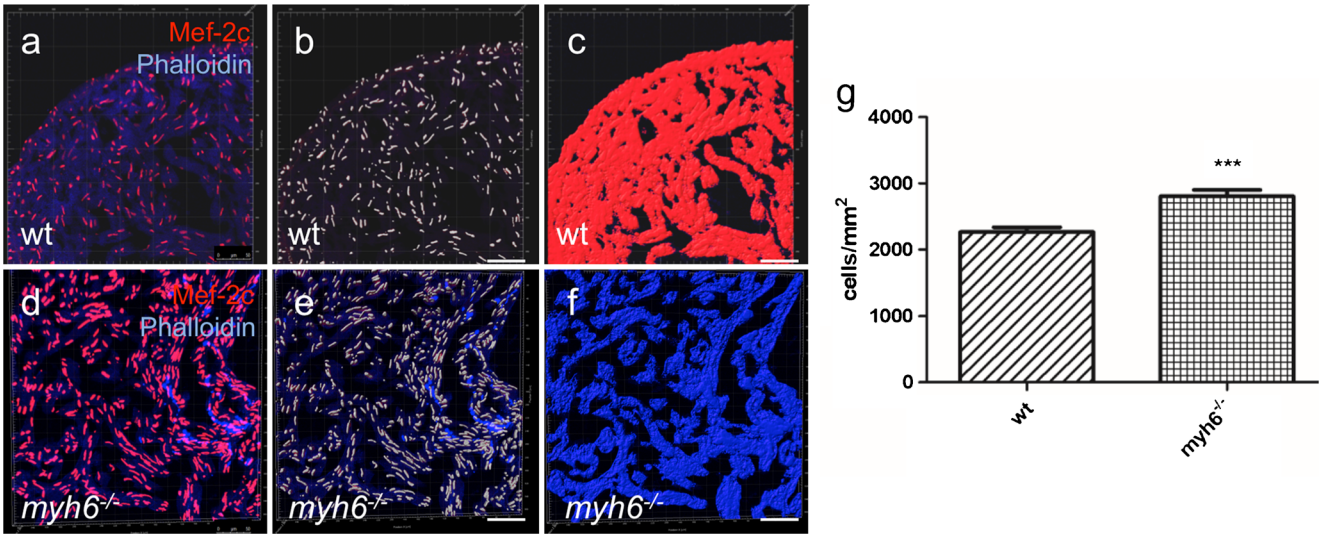


**Fig. 4** Ten-micrometer cryosections of adult zebrafish wild-type hearts (**a**) and *myh6*$^{-/-}$ (**d**) stained with the Mef-2c antibody. An example of the highlighting we used with the help of the Imaris program to measure the number of Mef-2c-positive nuclei. This is the measurement we used to count the cardiomyocyte cell number in wild-type (**b**) and *myh6*$^{-/-}$ (**e**). Highlighting the myocardial area (pseudocolored red or blue from Imaris using the original Alexa 633 phalloidine staining data from **a**, **d**) of the wild-type (**c**) and *myh6*$^{-/-}$ (**f**) myocardium surface area used to calculate cell density (**f**). Quantification (**g**) of the cell density between wild-type *myh6*$^{-/-}$ hearts (**b**/**c** and **e**/**f** respectively) shows a statistically significant difference ($p = 0.0016$, $n = 25$ cryosections from 7 fish per sample). Scale bars, 50 μm

As additional evidence of a hyperplastic response, we measured the ratio of Mef2$^{+}$PCNA$^{+}$/Mef2$^{+}$, which is an indicator of the proliferation of cardiomyocytes. We detected more proliferating cardiomyocytes in *myh6*$^{-/-}$ adult ventricles ($3.96 \pm 0.183$) than in wt ($2.05 \pm 0.073$) (Fig. 5, $p < 0.0001$, 5 wt and 5 *myh6*$^{-/-}$ ventricles were used for this experiment; wt 10 sections; *myh6*$^{-/-}$ 12 sections).

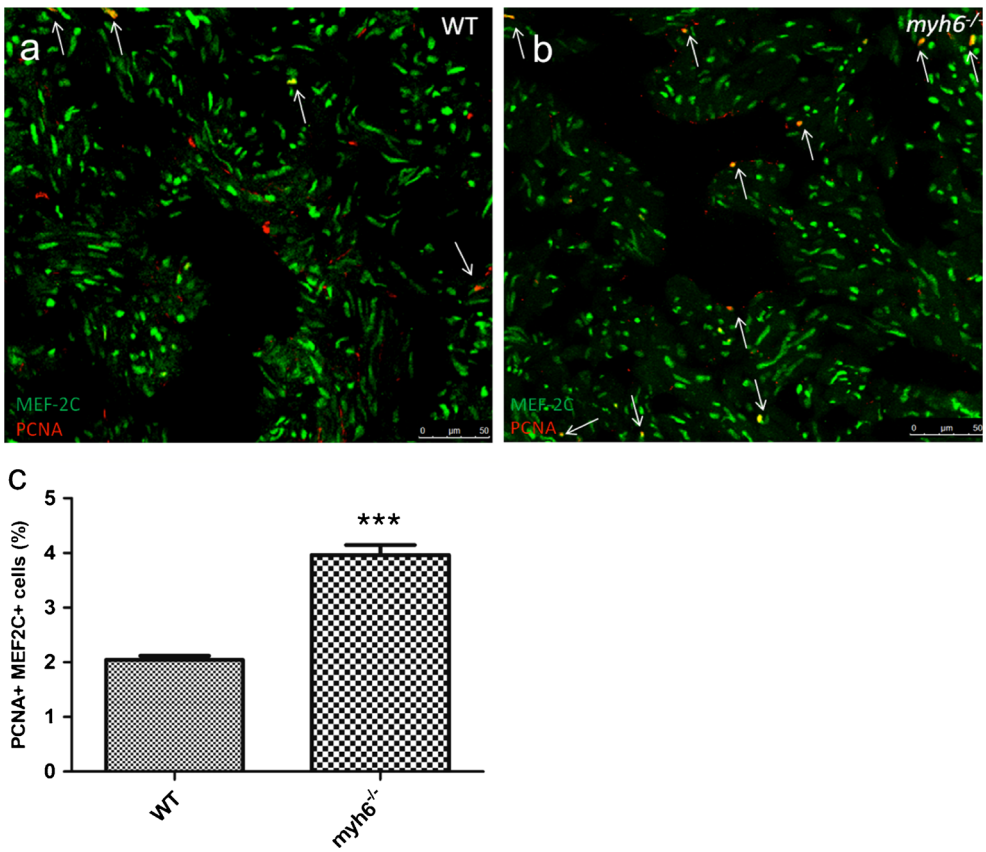


**Fig. 5** Ten-micrometer cryosections of adult zebrafish wild-type hearts (**a**) and *myh6*$^{-/-}$ (**b**) stained with proliferating cell nuclear antigen (PCNA) antibody (red) and Mef-2c antibody (green). Arrows show double staining PCNA$^{+}$ MEF2$^{+}$ (yellow-orange color). **c** Ratio of PCNA$^{+}$ MEF2$^{+}$ cells over total MEF2$^{+}$ cells between *myh6*$^{-/-}$ and wild-type hearts. A statistically significant difference is observed between the two groups ($p < 0.001$, $n = 10$ wt sections from 5 ventricles and $n = 12$ *myh6*$^{-/-}$ sections from 5 ventricles). Scale bars, 50 μm

### Upregulation of mammalian hypertrophy marker genes in the ventricles of 6-week-old mutants

The *nppa* (Natriuretic Peptide A) and *nppb* (Natriuretic Peptide B) genes are molecular markers of cardiomyocyte hypertrophy in mammals. The expression of these genes is upregulated in cases of increased heart size in zebrafish (Hendricks et al. 2009). We hence tested the expression levels of these genes in 6-week-old wild-type and *myh6*$^{-/-}$ hearts. The mRNA levels of these genes were higher in the *myh6*$^{-/-}$ samples. In particular, for the *nppa* gene, the increase in mRNA expression levels of the mutant hearts was 6.4 times relative to wild-type whereas for the *nppb* gene the increase was 6.86 times (Fig. 6a, nppa $p = 0.029$; 6b nppb = 0.004, $n = 6$ ventricles per group). Therefore, although the molecular signature of transcriptional activation indicates a hypertrophic response, mainly annotated as such from mammalian data, we only observed hyperplasia contributing to the ventricular enlargement and remodeling of *myh6*$^{-/-}$.

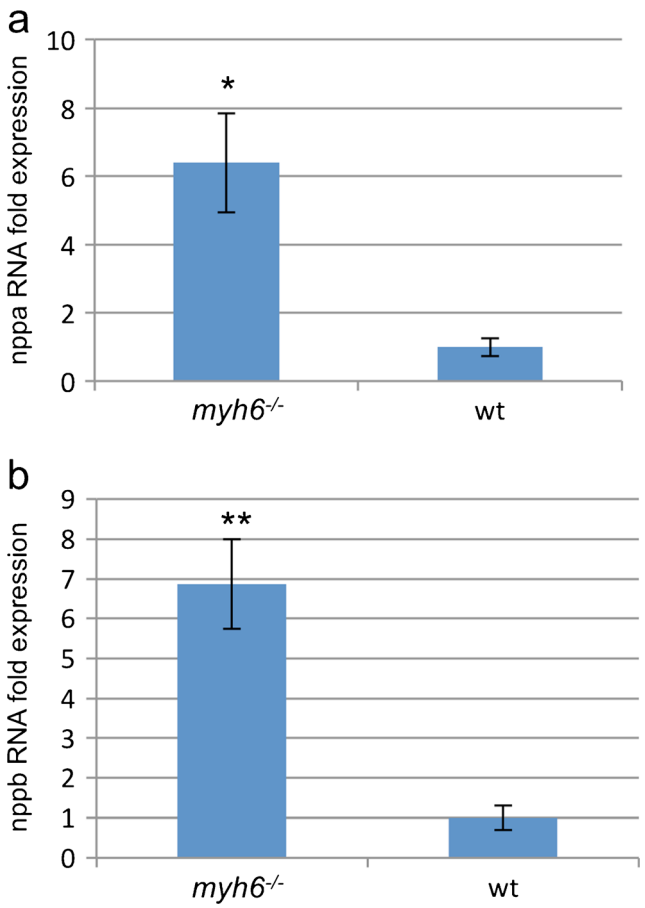


**Fig. 6** RNA expression levels of nppa (**a**) in the ventricles of 6-week *myh6*$^{-/-}$ and wild-type zebrafish. RNA expression levels of nppb (**b**) in the ventricles of 6-week *myh6*$^{-/-}$ and wild-type zebrafish. Both nppa and nppb RNA expression levels are upregulated in *myh6*$^{-/-}$ ventricles. $p < 0.05$ $n = 6$ ventricles per group

### Activation of ER-stress pathway

In an effort to better understand the pathophysiological mechanism of the ventricular overload response, we used western blot analysis to investigate some key markers of ER-stress activation. We found a 5.74-fold upregulation of Bip, the upstream activating factor of the ER-stress pathway, in the *myh6*$^{-/-}$ ventricle compared to wt ventricles, with a statistically significant difference ($p = 0.001$). Furthermore, in mutant ventricles, the p-eif2a levels were also elevated by 2.88 folds relative to wild-type ventricles, with a statistically significant difference ($p = 0.0049$). We used three different samples of *myh6*$^{-/-}$ and wild-type hearts and β-actin for the normalization (Fig. 7).

## Discussion

We analyzed the mechanisms involved in a genetic model of adult zebrafish ventricular remodeling. *myh6*$^{-/-}$ mutants survive with a single functioning chamber heart but increase the size of their ventricle as a response to a non-functional hypoplastic atrium. A hypertrophic response is responsible for the pathological increase in the heart size of mammals (Ahuja et al. 2007; Anversa et al. 2006). The majority of genetic DCM in mammals is autosomal dominantly inherited (Olivotto et al. 2015; McNally and Mestroni 2017). Here, we presented data that point to a hypertrophy-related transcriptional response of adult *myh6*$^{-/-}$ hearts. This includes the molecular markers (nppa/b). However, histological analyses of adult *myh6*$^{-/-}$ showed that the enlargement of the ventricle is predominantly due to hyperplasia. Under chronic hemodynamic overload, cardiac nppa and nppb synthesis and secretion increases. This increase is seen as a cardioprotective mechanism, given the beneficial effects of nppa and nppb on cardiac preload, afterload and cardiovascular growth (McGrath et al. 2005). Additionally, the ER-stress pathway has further cardioprotective action. Specifically, PERK (same pathway with p-eif2a) overexpression promotes cell survival under hypoxic conditions (Lu et al. 2004). Phosphorylation of eIF2α is an early event observed in cardiomyocytes after ischemia in vitro and after I/R in vivo (Szegezdi et al. 2006; Miyazaki et al. 2011). The cardioprotective effects of the UPR can be attributed to the induction of ER chaperones and the consequent enhancement of protein folding (Glembotski 2008). We should also highlight that molecular markers of cardiomyocyte hypertrophy being involved in hyperplastic processes are in accordance with the findings of Becker et al. (2011). Further dissection of the transcriptomic profile of adult *myh6*$^{-/-}$ ventricles will hopefully answer what molecular mechanisms differentiate the zebrafish cardiomyocytes' response from the mammalian ones.

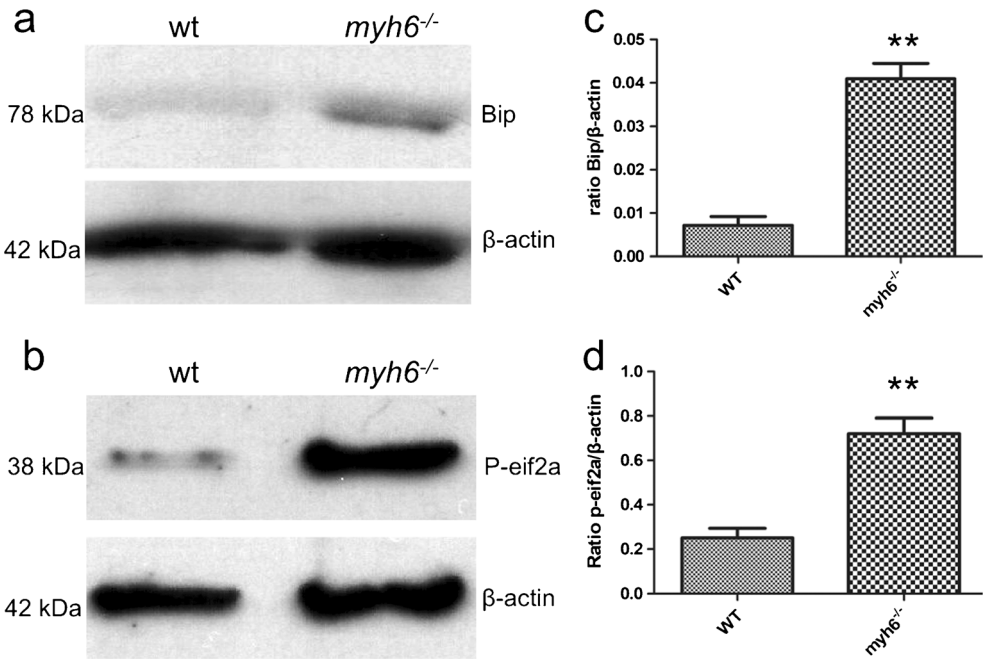


**Fig. 7** **a**, **b** Western blot using wild-type and *myh6*$^{-/-}$ adult zebrafish ventricles. We investigated the expression levels of proteins involved in the ER-stress pathway (Bip, p-eif2a) (**c**, **d**). Western blot analysis showed a statically significant difference of Bip ($p = 0.001$) and p-eif2a ($p = 0.004$) expression in mutant zebrafish compared to wild-type animals ($n = 3$ per group).

In parallel, it is noteworthy the transdifferentiation of atrial cardiomyocytes to elastin positive cells. Elastin is the predominant protein in the arterial wall and can contribute up to 50% of its dry weight (Karnik et al. 2003). Elastin also confers elasticity, preventing tissue tearing by mechanical stretching underload (Patel et al. 2006) and is the polymeric extracellular matrix protein that provides the properties of extensibility and elastic recoil to large arteries, lung parenchyma, elastic ligaments, elastic cartilages, skin and other elastic tissues of all vertebrates with the exception of the agnathans (Miao et al. 2007). Due to the genetic mutation in *amhc*, the *myh6*$^{-/-}$ atrial cardiomyocytes could not contract. However, it appears that upon the long-term dynamic stimulation of hemodynamic flow elastin biosynthesis was promoted as previously described in a different system (Isenberg 2003). It has also been found that PGA scaffolds promote the production of elastin by a dynamic stimulation (Kim et al. 1999). The biomechanical forces associated with contractility and blood flow have been suggested to play important roles in driving multiple aspects of cardiac morphogenesis. Alterations in circulation, as observed in *wea* mutants, can trigger cardiac remodeling and valve defects (Bartman and Hove 2005; Hove et al. 2003; Kalogirou et al. 2014). Therefore, a possible mechanism for depositing elastin is the change of hemodynamics in the atrium. The final result is the strengthening of the wall of the hypoplastic atrium so as to withstand the blood flow, simulating a blood vessel.

The elastin deposition in the atrium compensates for the lack of the Myh6 protein, sustaining a life-compatible, functional heart state and is analogous to the regeneration after ventricular injury. This particular mutant can be used as a model to study the correlation between ER-stress and cardiovascular diseases. Numerous studies using pharmacological agents that directly modulate the UPR have been published and are shedding light on emerging and promising tools for the effective treatment of cardiovascular diseases (Wang et al. 2018). Furthermore, alterations in circulation, as observed in *wea* mutants, can trigger significant changes in chamber size, shape, cellular organization and gene expression, thus rendering this mutant a potentially useful tool in understanding congenital heart defects associated with blood flow obstruction (Berdougo et al. 2003; Singleman and Holtzman 2012). In conclusion, this case further establishes the vast abilities of zebrafish in the rehabilitation of cardiac defects and demonstrates its potential as an ideal model for the study of heart diseases.

**Acknowledgements** We would like to thank Prof. Neil Chi for providing the *Tg(amhc:eGFP)*$^{s958}$ and Prof. Fred Keely for the elastin antibody.

**Funding** This study was funded by the Greek General Secreteriat for Research and Development European Social Fund, the European Union and National Funds (Aristia I, zfValves -270 grant to DB).

## Compliance with ethical standards

**Conflict of interest** The authors declare that they have no conflict of interest.

## References

Ahuja P, Sdek P, MacLellan WR (2007) Cardiac myocyte cell cycle control in development, disease, and regeneration. Physiol Rev 87(2):521–544

Anversa P, Kajstura J, Leri A, Bolli R (2006) Life and death of cardiac stem cells: a paradigm shift in cardiac biology. Circulation 113(11): 1451–1463

Auman HJ, Coleman H, Riley HE, Olale F, Tsai HJ, Yelon D (2007) Functional modulation of cardiac form through regionally confined cell shape changes. PLoS Biol 5(3):e53

Bakkers J (2011) Zebrafish as a model to study cardiac development and human cardiac disease. Cardiovasc Res 91(2):279–288

Bartman T, Hove J (2005) Mechanics and function in heart morphogenesis. Dev Dyn 233(2):373–381

Becker JR, Deo RC, Werdich AA, Panakova D, Coy S, MacRae CA (2011) Human cardiomyopathy mutations induce myocyte hyperplasia and activate hypertrophic pathways during cardiogenesis in zebrafish. Dis Model Mech 4(3):400–410

Beis D, Bartman T, Jin SW, Scott IC, D'Amico LA, Ober EA, Verkade H, Frantsve J, Field HA, Wehman A, Baier H, Tallafuss A, Bally-Cuif L, Chen JN, Stainier DY, Jungblut B (2005) Genetic and cellular analyses of zebrafish atrioventricular cushion and valve development. Development 132(18):4193–4204

Berdougo E, Coleman H, Lee DH, Stainier DY, Yelon D (2003) Mutation of weak atrium/atrial myosin heavy chain disrupts atrial function and influences ventricular morphogenesis in zebrafish. Development 130(24):6121–6129

Bertolotti A, Zhang Y, Hendershot LM, Harding HP, Ron D (2000) Dynamic interaction of Bip and ER stress transducers in the unfolded-protein response. Nat Cell Biol 2:326–332

Bournele D, Beis D (2016) Zebrafish models of cardiovascular disease. Heart Fail Rev (6):803–813

Chico TJ, Ingham PW, Crossman DC (2008) Modeling cardiovascular disease in the zebrafish. Trends Cardiovasc Med 18(4):150–155

Engel FB, Schebesta M, Duong MT, Lu G, Ren S, Madwed JB, Jiang H, Wang Y, Keating MT (2005) p38 MAP kinase inhibition enables proliferation of adult mammalian cardiomyocytes. Genes Dev 19(10):1175–1187

Foglia MJ, Poss K (2016) Building and re-building the heart by cardiomyocyte proliferation. Development 143(5):729–740

Glembotski CC (2008) The role of the unfolded protein response in the heart. J Mol Cell Cardiol 44:453–459

Hendricks M, Sun X, Hoage T, Bai P, Ding Y, Chen Z, Zhang R, Huang W, Jahangir A, Paw B (2009) Cardiac hypertrophy involves both myocyte hypertrophy and hyperplasia in anemic zebrafish. PLoS One 4(8):e6596

Hove JR, Koster RW, Forouhar AS, Acevedo-Bolton G, Fraser SE, Gharib M (2003) Intracardiac fluid forces are an essential epigenetic factor for embryonic cardiogenesis. Nature 421:172–177

Howe K, Clark MD, Torroja CF, Torrance J, Berthelot C, Muffato M, Collins JE, Humphray S, McLaren K, Matthews L, McLaren S, Sealy I, Caccamo M, Churcher C, Scott C, Barrett JC, Koch R, Rauch GJ, White S, Chow W, Kilian B, Quintais LT, Guerra-Assunção JA, Zhou Y, Gu Y, Yen J, Vogel JH, Eyre T, Redmond S, Banerjee R, Chi J, Fu B, Langley E, Maguire SF, Laird GK, Lloyd D, Kenyon E, Donaldson S, Sehra H, Almeida-King J, Loveland J, Trevanion S, Jones M, Quail M, Willey D, Hunt A, Burton J, Sims S, McLay K, Plumb B, Davis J, Clee C, Oliver K, Clark R, Riddle C, Elliot D, Threadgold G, Harden G, Ware D, Begum S, Mortimore B, Kerry G, Heath P, Phillimore B, Tracey A, Corby N, Dunn M, Johnson C, Wood J, Clark S, Pelan S, Griffiths G, Smith M, Glithero R, Howden P, Barker N, Lloyd C, Stevens C, Harley J, Holt K, Panagiotidis G, Lovell J, Beasley H, Henderson C, Gordon D, Auger K, Wright D, Collins J, Raisen C, Dyer L, Leung K, Robertson L, Ambridge K, Leongamornlert D, McGuire S, Gilderthorp R, Griffiths C, Manthravadi D, Nichol S, Barker G, Whitehead S, Kay M, Brown J, Murnane C, Gray E, Humphries M, Sycamore N, Barker D, Saunders D, Wallis J, Babbage A, Hammond S, Mashreghi-Mohammadi M, Barr L, Martin S, Wray P, Ellington A, Matthews N, Ellwood M, Woodmansey R, Clark G, Cooper J, Tromans A, Grafham D, Skuce C, Pandian R, Andrews R, Harrison E, Kimberley A, Garnett J, Fosker N, Hall R, Garner P, Kelly D, Bird C, Palmer S, Gehring I, Berger A, Dooley CM, Ersan-Ürün Z, Eser C, Geiger H, Geisler M, Karotki L, Kirn A, Konantz J, Konantz M, Oberländer M, Rudolph-Geiger S, Teucke M, Lanz C, Raddatz G, Osoegawa K, Zhu B, Rapp A, Widaa S, Langford C, Yang F, Schuster SC, Carter NP, Harrow J, Ning Z, Herrero J, Searle SM, Enright A, Geisler R, Plasterk RH, Lee C, Westerfield M, de Jong PJ, Zon LI, Postlethwait JH, Nüsslein-Volhard C, Hubbard TJ, Roest Crollius H, Rogers J, Stemple DL (2013) The zebrafish reference genome sequence and its relationship to the human genome. Nature 496(7446):498–503

Isenberg BC (2003) Tranquillo RT (2003) long-term cyclic distention enhances the mechanical properties of collagen-based media equivalents. Ann Biomed Eng 31:937–949

Kalogirou S, Malissovas N, Moro E, Argenton F, Stainier DY, Beis D (2014) Intracardiac flow dynamics regulate atrioventricular valve morphogenesis. Cardiovasc Res 104(1):49–60

Karnik SK, Brooke BS, Antonio BG, Sorensen L, Wythe JD, Schwartz RS, Keating MT, Li DY (2003) A critical role for elastin signaling in vascular morphogenesis and disease. Development 130(2):411–423

Kikuchi K, Holdway JE, Major RJ, Blum N, Dahn RD, Begemann G, Poss KD (2011) Retinoic acid production by endocardium and epicardium is an injury response essential for zebrafish heart regeneration. Dev Cell 20(3):397–404

Kim BS, Nikolovski J, Bonadio J, Mooney DJ (1999) Cyclic mechanical strain regulates the development of engineered smooth muscle tissue. Nat Biotechnol 17:979–983

Lee AS (2005) The ER chaperone and signaling regulator GRP78/bip as a monitor of endoplasmic reticulum stress. Methods 35:378–381

Li FWX, Bunger PC, Gerdes AM (1997) Formation of binucleated cardiac myocytes in rat heart: I., role of actin-myosin contractile ring. J Mol Cell Cardiol 29:1541–1551

Lu PD, Jousse C, Marciniak SJ, Zhang Y, Novoa I, Scheuner D, Kaufman RJ, Ron D, Harding HP (2004) Cytoprotection by pre-emptive conditional phosphorylation of translation initiation factor 2. EMBO J 23:169–179

McGrath MF, de Bold ML, de Bold AJ (2005) The endovrine function of the heart. Trends Emdrocrinol Metab 16(10):469–477

McNally EM, Mestroni L (2017) Dilated cardiomyopathy: genetic determinants and mechanisms. Circ Res 121(7):731–748

Miao M, Bruce AE, Bhanji T, Davis EC, Keeley FW (2007) Differential expression of two tropoelastin genes in zebrafish. Matrix Biol 26(2): 115–124

Miyazaki Y, Kaikita K, Endo M, Horio E, Miura M, Tsujita K, Hokimoto S, Yamamuro M, Iwawaki T, Gotoh T, Ogawa H, Oike Y (2011) C/EBP homologous protein deficiency attenuates myocardial reperfusion injury by inhibiting myocardial apoptosis and inflammation. Arterioscler Thromb Vasc Biol 31:1124–1132

Nemtsas P, Wettwer E, Christ T, Weidinger G, Ravens U (2010) Adult zebrafish heart as a model for human heart? An electrophysiological study. J Mol Cell Cardiol 48(1):161–171

Okada K, Minamino T, Tsukamoto Y, Liao Y, Tsukamoto O, Takashima S, Hirata A, Fujita M, Nagamachi Y, Nakatani T, Yutani C, Ozawa K, Ogawa S, Tomoike H, Hori M, Kitakaze M (2004) Prolonged endoplasmic reticulum stress in hypertrophic and failing heart after aortic constriction: possible contribution of endoplasmic. Circulation 110:705–712

Olivetti G, Maestri R, Corradi D, Lagrasta C, Gambert SR, Anversa P (1996) Aging, cardiac hypertrophy and ischemic cardiomyopathy do not affect the proportion of mononucleated and multinucleated myocytes in the human heart. J Mol Cell Cardiol 28:1463–1477

Olivotto I, d'Amati G, Basso C, Van Rossum A, Patten M, Edmin PY, Tomberli B, Camici PG, Michels M (2015) Defining phenotypes and disease progression in sarcomeric cardiomyopathies; contemporary role of clinical investigations. Cardiovasc Res 105(4):409–423

Patel A, Fine B, Sandig M, Mequanint K (2006) Elastin biosynthesis: the missing link in tissue-engineered blood vessels. Cardiovasc Res 71(1):40–49

Poss KD, Wilson LG, Keating MT (2002) Heart regeneration in zebrafish. Science 298(5601):2188–2190

Rivello HG, Meckert PC, Vigliano C, Favaloro R, Laguens RP (2001) Cardiac myocyte nuclear size and ploidy status decrease after mechanical suport. Cardiovasc Pathol 10:53–57

Sedmera D, Hu N, Weiss KM, Keller BB, Denslow S, Thompson RP (2002) Cellular changes in experimental left heart hypoplasia. Anat Rec 267(2):137–145

Seidman JG, Seidman C (2001) The genetic basis for cardiomyopathy: from mutation identification to mechanistic paradigms. Cell 104: 557–567

Shih YH, Zhang Y, Ding Y, Ross CA, Li H, Olson TM, Xu X (2015) Cardiac transcriptome and dilated cardiomyopathy genes in zebrafish. Circ Cardiovasc Genet 8(2):261–269

Singleman C, Holtzman NG (2012) Analysis of postembryonic heart development and maturation in the zebrafish, Danio rerio. Dev Dyn : Off Publ Am Assoc Anatomists 241(12):1993–2004

Stainier DY (2001) Zebrafish genetics and vertebrate heart formation. Nat Rev Genet 2:39–48

Sun X, Hoage T, Bai P, Ding Y, Chen Z, Zhang R, Huang W, Jahangir A, Paw B, Li YG, Xu X (2009) Cardiac hypertrophy involves both myocyte hypertrophy and hyperplasia in anemic zebrafish. PLoS One 4(8):e6596. https://doi.org/10.1371/journal.pone.0006596

Szegezdi E, Duffy A, O'Mahoney ME, Logue SE, Mylotte LA, O'Brien T, Samali A (2006) ER stress contributes to ischemia-induced cardiomyocyte apoptosis. Biochem Biophys Res Commun 349:1406–1411

Wang J, Poss KD (2016) Methodologies for inducing cardiac injury and assaying regeneration in adult zebrafish. Methods Mol Biol 1451: 225–235

Wang S, Binder P, Fang Q, Wang Z, Xiao W, Liu W, Wang X (2018) Endoplasmic reticulum stress in the heart: insights into mechanisms and drug targets. Br J Pharmacol 175:1293–1304. https://doi.org/10.1111/bph.13888

Westerfield M (2000) The zebrafish book. A guide for the laboratory use of zebrafish (*Danio rerio*), 4th edn. Univ. of Oregon Press, Eugene

Wills AA, Holdway JE, Major RJ, Poss KD (2008) Regulated addition of new myocardial and epicardial cells fosters homeostatic cardiac growth and maintenance in adult zebrafish. Development 135(1): 183–192

Zebrowski DC, Engel FB (2013) The cardiomyocyte cell cycle in hypertrophy, tissue homeostasis, and regeneration. Rev Physiol Biochem Pharmacol 165:67–96

Zhang R, Han P, Yang H, Ouyang K, Lee D, Lin YF, Ocorr K, Kang G, Chen J, Stainier DY (2013) In vivo cardiac reprograming contributes to zebrafish heart regeneration. Nature 498(7455):497–501